PHYSICAL REVIEW A **91**, 061803(R) (2015)

Sub-Poissonian phonon lasing in three-mode optomechanics

Niels Lörch and Klemens Hammerer
Institut für Gravitationsphysik, Leibniz Universität Hannover and Max-Planck-Institut für Gravitationsphysik (Albert-Einstein-Institut), Callinstraße 38, 30167 Hannover, Germany
and Institut für Theoretische Physik, Leibniz Universität Hannover, Appelstraße 2, 30167 Hannover, Germany
(Received 2 March 2015; published 9 June 2015)

We propose to use the resonant enhancement of the parametric instability in an optomechanical system of two optical modes coupled to a mechanical oscillator to prepare mechanical limit cycles with sub-Poissonian phonon statistics. Strong single-photon coupling is not required. The requirements regarding sideband resolution, circulating cavity power, and environmental temperature are in reach with state of the art parameters of optomechanical crystals. Phonon antibunching can be verfied in a Hanburry Brown–Twiss measurement on the output field of the optomechanical cavity.

DOI: 10.1103/PhysRevA.91.061803 PACS number(s): 42.50.Wk, 07.10.Cm, 42.50.Ct, 42.65.−k

I. INTRODUCTION

Optomechanical experiments, where optical resonators are coupled to mechanical oscillators [1,2], are achieving increasingly good control of macroscopic objects on the quantum level: Milestones such as cooling the motion of these oscillators to their quantum ground state [3,4], coherent transfer of quantum states between light and mechanics [5,6], observation of radiation pressure shot noise on the oscillator [7,8], as well as entanglement between the light field and the mechanical oscillator [9] have been achieved in recent years. The phonon analog of a laser, which is realized using the optical cavity as the gain medium to excite coherent oscillations of the mechanical oscillator has been demonstrated in [10–18], and its phonon statistics has been mapped out via a Hanburry Brown–Twiss measurement on the sideband photons emitted from the optomechanical cavity [18].

Theoretical work suggests that it is possible to prepare a state with quantum signatures in the phonon statistics such as phonon antibunching and even negative Wigner density [19–24]. However, the requirements to see phonon antibunching scale unfavorably with the system parameters, so that sub-Poissonian phonon statistics has eluded experimental observation. In this Rapid Communication we propose to make use of the enhanced optomechanical nonlinearity [25–27] of a setup with two optical modes to overcome this difficulty and prepare phonon laser states featuring antibunching in steady state with state of the art optomechanical crystals.

The enhanced nonlinearity has been discussed in the context of detectors for phonons or photons [26], quantum memory [28], and to improve [27] the parameters of mechanically induced photon antibunching [29,30]. In the context of the phonon laser transition the enhanced optomechanical instability with two optical modes has been anticipated as a possible complication for gravitational wave detectors [31], and has been studied experimentally [11–15,32] and theoretically [33–38] in the classical regime. Here we show for that one can detect quantum signatures in the phonon lasing of such a three-mode system. In particular, antibunched statistics of the phonon number ($\hat{n} = c^\dagger c$), as commonly characterized by a Fano factor $F = \langle \Delta \hat{n}^2 \rangle / \langle \hat{n} \rangle < 1$, and a second order coherence function $g^{(2)}(t)$ at time $t = 0$,

$$g^{(2)}(0) = \langle c^\dagger c^\dagger c c \rangle / \langle \hat{n} \rangle^2 = 1 + (F - 1)/\langle \hat{n} \rangle < 1, \quad (1)$$

can be prepared in steady state. With more demanding system requirements, even a negative mechanical Wigner density can be achieved.

II. SYSTEM DESCRIPTION

We study the optomechanical setup depicted in Fig. 1. Two optical modes a and b couple to a mechanical mode c via the three-mode interaction Hamiltonian $V = g_0(ab^\dagger + a^\dagger b)(c + c^\dagger)$, where g_0 is the single-photon optomechanical coupling strength and a,b,c are the lowering operators of the different modes. Such an interaction has been implemented in Refs. [11–15,32]. The optical mode b is resonantly driven with a laser of power P, which we parametrize with $E = \sqrt{\kappa P/\hbar\omega_b}$ (κ is the cavity linewidth, and ω_b the resonance frequency of mode b). The other optical mode a is detuned with respect to cavity mode b and the driving laser by Δ, and the mechanical frequency is ω_m, so that the Hamiltonian in a rotating frame for both cavities with frequency ω_b is $H = H_0 + V + iE(b^\dagger - b)$ with $H_0 = \omega_m c^\dagger c - \Delta a^\dagger a$.

Depending on the sign of the laser detuning, the laser either cools the mechanical mode ($\Delta < 0$), or gives rise to self-induced mechanical oscillations ($\Delta > 0$). In the latter regime the intrinsic nonlinearity of the three-mode optomechanical interaction V stabilizes the mechanical oscillation at a finite amplitude [32]. We choose a detuning $\Delta = \omega_m$ between the two cavities which corresponds to a resonant excitation of

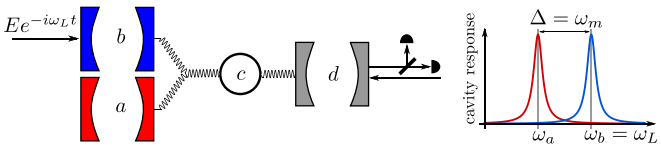

FIG. 1. (Color online) Left: Two optical modes a and b are coupled to a mechanical mode c. The b mode is resonantly driven by a laser of strength E and frequency $\omega_L = \omega_b$. The a mode is detuned from b by $\Delta = \omega_m$, the mechanical resonance frequency, as depicted in the plot on the right. The nonlinear interaction of the three modes a, b, and c gives rise to optomechanical limit cycles with strongly sub-Poissonian phonon number statistics. A third optical mode d can be used to reduce the effective temperature of the mechanical oscillator's bath and to read out the phonon statistics in a Hanburry Brown–Twiss measurement.

optomechanical limit cycles. In an interaction picture with respect to H_0 the Hamiltonian is

$$H_I = iE(b^\dagger - b) + g_0(ab^\dagger c + a^\dagger b c^\dagger). \tag{2}$$

We neglected here fast oscillating terms $e^{2i\omega_m t} g_0 a b^\dagger c^\dagger + \text{H.c.}$, assuming a cavity decay rate of $\kappa \ll \omega_m$ for both cavities (the corrections are of order κ^2/ω_m^2, i.e., negligible for typical optomechanical crystals). In the framework of Langevin equations the system dynamics is then described by

$$\begin{aligned} \dot{a} &= -ig_0 bc^\dagger - \frac{\kappa}{2}a + \sqrt{\kappa}a_{\text{in}}, \\ \dot{b} &= -ig_0 ac - \frac{\kappa}{2}b + E + \sqrt{\kappa}b_{\text{in}}, \end{aligned} \tag{3}$$

$$\dot{c} = -ig_0 a^\dagger b - \frac{\gamma}{2}c + \sqrt{\gamma}c_{\text{in}}, \tag{4}$$

where $\langle a_{\text{in}}(t)a_{\text{in}}^\dagger(t')\rangle = \langle b_{\text{in}}(t)b_{\text{in}}^\dagger(t')\rangle = \delta(t-t')$ and $\langle c_{\text{in}}(t)c_{\text{in}}^\dagger(t')\rangle = (1+\bar{n})\delta(t-t')$ are the two-time correlation functions of the Langevin noise forces. We assumed energy decay of the mechanical oscillator at rate γ, due to coupling to a thermal thermal bath with mean occupation $\bar{n}$ [39].

III. CALCULATION OF CLASSICAL AMPLITUDES

We express each operator as a sum of a classical ($\mathbb{C}$ number) component and an operator describing fluctuations around it, such that $a = \alpha + \delta a$, $b = \beta + \delta b$, and $c = \zeta + \delta c$. Inserting this into the Langevin equations, and considering the $\mathbb{C}$-number components only, gives rise to a coupled set of nonlinear equations for the classical cavity amplitudes α and β, and the (complex) mechanical amplitude ζ. In particular, one finds $\dot{\alpha} = -ig_0\beta\zeta^* - \frac{\kappa}{2}\alpha$ and $\dot{\beta} = -ig_0\alpha\zeta - \frac{\kappa}{2}\beta + E$. We assume that the optical amplitudes adiabatically follow the motion of the mechanical oscillator which is equivalent to the conditions $(\bar{n}+1)\gamma, g_0|\alpha|, g_0|\beta| \ll \kappa$. Solving $\dot{\alpha} = \dot{\beta} = 0$ results in the adiabatic solution for the optical amplitudes

$$\begin{aligned} \beta(\zeta,\zeta^*) &= \frac{E\kappa}{2h_\zeta}, \\ \alpha(\zeta,\zeta^*) &= -i\frac{Eg_0\zeta^*}{h_\zeta}, \end{aligned} \tag{5}$$

where $h_\zeta = g_0^2|\zeta|^2 + \frac{1}{4}\kappa^2$. Inserting these optical amplitudes in the equation of motion for the classical mechanical amplitude results in $\dot{\zeta} = -\frac{1}{2}(\gamma + \gamma_{\text{opt}})\zeta$, where the optically mediated (anti)damping is

$$\gamma_{\text{opt}}(\zeta) = -\frac{g_0^2 E^2 \kappa}{h_\zeta^2} \tag{6}$$

[cf. Fig. 2(a)]. γ_{opt} is negative for all mechanical amplitudes and its absolute value decreases with increasing amplitude ζ according to the Lorentzian given by h_ζ^2, approaching 0 for $\zeta \gg \kappa/g_0$. In agreement with [32] we define the dimensionless parameter $\mathcal{R} = \frac{|\gamma_{\text{opt}}(0)|}{\gamma} = \frac{16g_0^2E^2}{\kappa^3\gamma}$, which corresponds to the gain of mechanical amplification at zero mechanical amplitude. For $\mathcal{R} < 1$ the total mechanical damping $\gamma + \gamma_{\text{opt}}(0) > 0$ is positive for all amplitudes, implying $\zeta = 0$ in steady state. Above threshold, $\mathcal{R} > 1$, the steady state ($\dot{\zeta} = 0$) is achieved

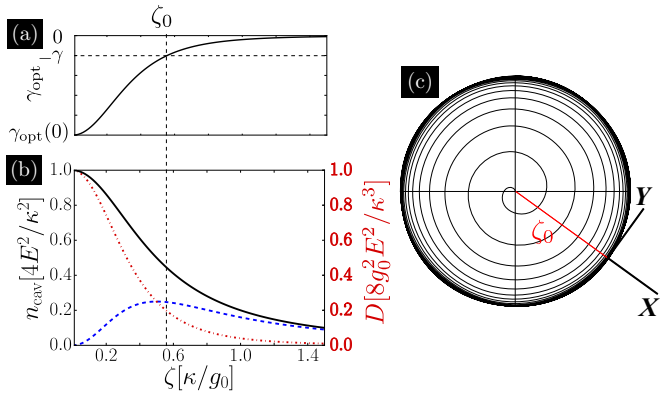

FIG. 2. (Color online) (a) Optically mediated (anti)damping $\gamma_{\text{opt}}(\zeta)$ (bold line) as a function of mechanical amplitude ζ according to Eq. (6). The steady state ζ_0 is reached when $\gamma_{\text{opt}}(\zeta_0) = -\gamma$ (dashed line). (b) Intracavity photon number $|\alpha|^2$ in mode a (blue dashed line), $|\beta|^2$ in mode b (red dash-dotted line), and total photon number $n_{\text{cav}} = |\alpha|^2 + |\beta|^2$ (black solid line) is plotted as a function of mechanical amplitude ζ according to Eq. (5). The optically induced diffusion $D_{\text{opt}} = g_0^2\frac{\kappa}{2}(|\alpha|^2 + |\beta|^2)/h_\zeta$ of the mechanical oscillator scales exactly like the red dash-dotted line with a scale as given on the right y axis. (c) Schematic phase space trajectory of the mechanical oscillator approaching the limit cycle attractor with amplitude ζ_0. In the corotating frame of the oscillator the X quadrature relates to its amplitude and the Y quadrature to its phase.

for a mechanical amplitude ζ_0 such that $\gamma_{\text{opt}}(\zeta_0) = -\gamma$ [cf. Fig. 2(a)]. The solution of this nonlinear equation is

$$|\zeta_0|^2 = \left(\frac{\kappa}{2g_0}\right)^2(\sqrt{\mathcal{R}} - 1). \tag{7}$$

The solution is unique (up to the oscillator's phase, where we choose $\zeta_0 = |\zeta_0|$, without loss of generality) and fully determined by the gain parameter $\mathcal{R}$ and the single-photon strong-coupling parameter $2g_0/\kappa$. It is instructive to contrast this result with the equivalent one for a conventional two-mode (one mechanical and one optical mode) optomechanical system where the mean phonon number of self-induced limit cycles scales as the inverse of the much smaller ratio $(g_0/\omega_m)^2$ instead. In view of Eq. (1) it is clear that a small oscillation amplitude is advantageous in order to observe strong antibunching and that the three-mode setup improves the signal approximately by a factor of $4(\omega_m/\kappa)^2$. This can be two orders of magnitude for typical system parameters of optomechanical crystals, e.g., $4(\omega_m/\kappa)^2 = 217$ with $\kappa/2\pi = 500$ MHz and $\omega_m/2\pi = 3.68$ GHz from [4].

IV. CALCULATION OF QUANTUM AMPLITUDE NOISE

The fluctuations δa, δb, and δc with respect to these classical amplitudes fulfill the linearized Langevin equations

$$\delta\dot{a} = \left(-\frac{\kappa}{2}\delta a - ig_0\zeta_0\delta b\right) - ig_0\beta_0\delta c^\dagger + \sqrt{\kappa}a_{\text{in}}, \tag{8}$$

$$\delta\dot{b} = \left(-\frac{\kappa}{2}\delta b - ig_0\zeta_0\delta a\right) - ig_0\alpha_0\delta c + \sqrt{\kappa}b_{\text{in}}, \tag{9}$$

$$\delta\dot{c} = -\frac{\gamma}{2}\delta c - ig_0(\alpha_0^*\delta b + \beta_0\delta a^\dagger) + \sqrt{\gamma}c_{\text{in}}, \tag{10}$$

where we consistently dropped all terms of quadratic order in the fluctuations. This approximation is only valid for large enough amplitudes. We also introduce here the shorthand notation $(\alpha_0,\beta_0)=(\alpha(\zeta_0),\beta(\zeta_0))$ for the cavity amplitudes in the developed mechanical limit cycle. The quantum fluctuations of the cavity modes can now be treated in analogy to the classical amplitudes simply by setting $\delta\dot{a}=\delta\dot{b}=0$ and solving the resulting algebraic equation. Inserting the solutions for δa and δb back into Eq. (10) gives the dynamics for the mechanical mode δc. For the canonical mechanical quadratures $X=(\delta c+\delta c^\dagger)/\sqrt{2}$ and $Y=(\delta c-\delta c^\dagger)/\sqrt{2}i$ [cf. Fig. 2(c)], we get effective Langevin equations

$$\dot{X}=-\tfrac{1}{2}\Gamma X+\sqrt{D}X_N,\quad \dot{Y}=\sqrt{D}Y_N, \tag{11}$$

with damping Γ, diffusion D, and noise forces fulfilling $\langle X_N(t),X_N(t')\rangle=\delta(t-t')$ and $\langle Y_N(t),Y_N(t')\rangle=\delta(t-t')$. Both $\Gamma=\gamma+\Gamma_{\rm opt}(\zeta)$ and $D=\gamma(\frac{1}{2}+\bar{n})+D_{\rm opt}(\zeta)$ have an intrinsic mechanical constant contribution and an optically mediated nonlinear (ζ-dependent) contribution. We find that $D_{\rm opt}(\zeta)=g_0^2\frac{\kappa}{2}(|\alpha|^2+|\beta|^2)/h_\zeta$ at the point of the limit cycle is exactly as large as the vacuum contribution of the mechanical bath, i.e., $D_{\rm opt}(\zeta_0)=\frac{\gamma}{2}$, but $\Gamma_{\rm opt}(\zeta_0)=\gamma(3-4/\sqrt{\mathcal{R}})$ can grow up to three times the mechanical damping for large $\mathcal{R}$. In total the damping and diffusion depicted in Figs. 2(a) and 2(b) are at the limit cycle

$$\Gamma(\zeta_0)=4\gamma(1-1/\sqrt{\mathcal{R}}),\quad D(\zeta_0)=\gamma(\bar{n}+1). \tag{12}$$

As schematically depicted in Fig. 2(c), in our convention the Y quadrature relates to the phase of the mechanical oscillator, which is subjected to undamped diffusion [cf. Eq. (11)]. The X quadrature relates to the mechanical amplitude, our focus of interest in this Rapid Communication. In particular, for the phonon occupation number $\hat{n}=c^\dagger c$ one finds $\langle\hat{n}\rangle=\zeta^2+\mathcal{O}(\zeta^0)$ and $\langle\hat{n}^2\rangle=\zeta^4+2\zeta^2\langle X^2\rangle+\mathcal{O}(\zeta^0)$, such that the Fano factor is $F\simeq 2\langle X^2\rangle$. Equation (11) gives $\langle X^2\rangle=D/\Gamma$ in steady state, i.e., the amplitude variance is determined by the compromise of diffusion and effective damping, yielding for the Fano factor

$$F=\frac{1}{2}\frac{1+\bar{n}}{1-1/\sqrt{\mathcal{R}}}. \tag{13}$$

This is in excellent agreement with numerical results shown in Fig. 4(a) that were obtained by Monte Carlo simulation (see Appendix) of a master equation equivalent to the exact, nonlinear equations of motion in Eqs. (3) and (4).

From Eq. (13) we see that for $\mathcal{R}\gg 1$ the Fano factor approaches $(1+\bar{n})/2$. Therefore, we arrive at the condition $\bar{n}<1$ necessary in order to observe sub-Poissonian phonon statistics. For a cryogenically cooled mechanical oscillator $\bar{n}=1/(e^{\hbar\omega_m/k_BT}-1)<1$ can in principle be achieved for a sufficiently high resonance frequency and at low temperature T (see [40,41]). However, in the present case it is possible to take advantage of laser cooling of the mechanical oscillator [42,43] in order to observe sub-Poissonian statistics.

V. ADDITIONAL LASER COOLING

Consider a setup where the mechanical oscillator is coupled to a third optical cavity of linewidth κ_d which is driven below resonance such as to induce an additional damping γ_L of the oscillator. Eliminating this cooling cavity gives rise to a "dressed" mechanical oscillator whose equation of motion is still given by (4) with an effective mechanical damping and occupation number

$$\gamma=\gamma_0+\gamma_L,\quad \bar{n}=\frac{\gamma_0\bar{n}_0+\gamma_L\bar{n}_L}{\gamma_0+\gamma_L}. \tag{14}$$

Here γ_0 is the linewidth and $\bar{n}_0$ the occupation number of the bare mechanical resonance (without laser cooling), and $\bar{n}_L=(\kappa_d/4\omega_m)^2$ is the quantum limit of optomechanical laser cooling [42,43].

In order to have $F<1$ we assume laser cooling to an effective phonon occupation $\bar{n}<1$. This comes at the cost of a decreased gain parameter $\mathcal{R}=16g_0^2E^2/\kappa^3(\gamma_0+\gamma_L)$, which can be compensated for by a somewhat more intense driving field. It is rather remarkable that laser cooling can help to observe a quantum feature such as sub-Poissonian phonon statistics: While laser cooling can provide a small effective occupation number $\bar{n}\ll\bar{n}_0$ it does so by increasing the effective mechanical linewidth $\gamma\gg\gamma_0$ by the same factor. As a result, the decoherence rate relevant for quantum effects, $\gamma_0\bar{n}_0=\gamma\bar{n}$, stays constant, such that laser cooling in most cases does not help in order to achieve quantum effects with mechanical oscillators.

VI. EXPERIMENTAL FEASIBILITY

The requirements on the system parameters to have $g^{(2)}(0)<1$ (and therefore $F<1$) is found by inserting the mean amplitude (7) and the Fano factor (13) in the definition

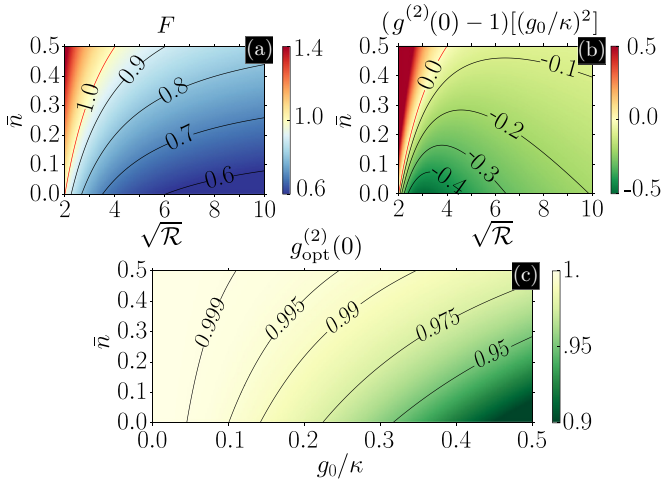

FIG. 3. (Color online) (a) Fano factor as a function of effective mechanical bath occupation number $\bar{n}$ and total number of photons in the cavity $n_{\rm ph}[\kappa\gamma/4g_0^2]=\sqrt{\mathcal{R}}$ according to Eq. (13). (b) Plot of $[g^{(2)}(0)-1][(g_0/\kappa)^2]$ as a function of the same parameters in units of the squared single-photon strong-coupling parameter $(g_0/\kappa)^2$ according to Eqs. (15) and (16). The condition for both sub-Poissonian statistics ($F<1$) and antibunching [$g^{(2)}(0)<1$] is visualized by the red contour line $\bar{n}=1-2/\sqrt{\mathcal{R}}$ in both plots. (c) Plot of $g^{(2)}_{\rm opt}(0)$ for optimal choice of $\mathcal{R}$ as a function of g_0/κ and $\bar{n}$ according to Eq. (17). All units in this figure are dimensionless.

(1) of $g^{(2)}(0)$,

$$g^{(2)}(0) - 1 = 4\left(\frac{g_0}{\kappa}\right)^2 \frac{F-1}{\sqrt{\mathcal{R}}-1}. \tag{15}$$

For the discussion of experimental feasibility it is more instructive to express the gain parameter $\mathcal{R}$ in terms of the steady state total number of photons in the cavity $n_{\rm ph} = |\alpha_0|^2 + |\beta_0|^2 = \frac{\kappa\gamma}{4g_0^2}\sqrt{R}$, where we used Eqs. (7) and (5). The circulating number of photons is important as it determines the heating of the mechanical structure, which was the limiting decoherence mechanism in recent experiments with optomechanical crystals [4]. In Figs. 3(a) and 3(b) we show the Fano factor F and $g^{(2)}(0) - 1$ (in units of g_0^2/κ^2) as a function of the number of photons in the cavity $n_{\rm ph}$ and the effective mechanical bath occupation number $\bar{n}$. In view of the dependence of the Fano factor and the second order coherence function on $\mathcal{R}$ [cf. Eqs. (13) and (15), respectively], it is clear that there is an optimal number of circulating photons minimizing $g^{(2)}(0)$ for given $\bar{n}$ and single-photon strong-coupling parameter g_0/κ. The minimum is reached at

$$n_{\rm ph}\left[\kappa\gamma/4g_0^2\right] = (3+\bar{n})/(1-\bar{n}) \tag{16}$$

and is given by

$$g^{(2)}_{\rm opt}(0) = 1 - \frac{1}{2}\left(\frac{g_0}{\kappa}\right)^2 \frac{(1-\bar{n})^2}{(1+\bar{n})}, \tag{17}$$

which is illustrated in Fig. 3(c). Thus, a large single-photon coupling helps, but is not strictly required, to create a robust signal to verify antibunching. We conclude that a sub-Poissonian phonon laser state can be prepared and verified outside the single-photon strong-coupling regime and for small but finite effective [cf. Eq. (14)] bath occupation $\bar{n}$ by detecting photon antibunching in the reflected light. We emphasize that phonon antibunching can be observed already in a regime of few circulating photons $n_{\rm ph} \ll 1$.

VII. READOUT OF PHONON STATISTICS

The readout of the—possibly antibunched—phonon statistics can be implemented in analogy to [18] using the cooling laser mode d. In the sideband resolved ($\kappa_d \ll \omega_m$) and linear ($g_d\zeta \ll \omega_m$) regime the dynamics of laser cooling can be understood as a continuous coherent state swap interaction $cd^\dagger + c^\dagger d$ [5,6]. The phonon statistics of d can then be measured by counting the photons in the output of the cooling cavity d at the sideband frequency $+\omega_m$ [18]. Hence with this readout scheme phonon antibunching is detected via photon antibunching.

Note that detection losses of an experiment do not alter the measured second order coherence function, as both its numerator $\langle c^\dagger c^\dagger cc\rangle$ and denominator $\langle\hat{n}\rangle^2$ scale with the detection efficiency squared. Additional noise counts however, mostly caused by dark counts from the detector and carrier photons leaking through the frequency filter, will bring $g^{(2)}(0)$ closer to one. In [18] the noise equivalent-phonon number $n_{\rm NEP}$, defined as the ratio of noise counts and sideband counts per phonon, was limited by $n_{\rm NEP} = 0.89$. Using an additional filter to decrease the carrier bleed through, the authors even expect to improve this value by a few orders of magnitude. We conclude that a phonon statistics readout that does not significantly alter $g^{(2)}(0)$ is feasible.

VIII. EXPERIMENTAL CASE STUDY

Currently the highest reported value for the coupling in optomechanical crystals is $g_0/2\pi = 1.1$ MHz [44]. The lowest cavity decay rate in a photonic crystal is, to our knowledge, $\kappa = 20$ MHz [45]. While the best ratio achieved in a single device is $g_0/\kappa = 0.007$ [4], combining the best values in one device would already reach $g_0/\kappa \approx 0.055$. The lowest reported effective bath occupation reached with optomechanical cooling is $\bar{n} = 0.85$ [4]; using a dilution refrigerator mechanical oscillators have even been cooled down below $\bar{n} < 0.07$. Assuming a slightly more optimistic $g_0/\kappa = 0.1$, an effective environmental temperature of 200 mK, and a mechanical frequency of 5 GHz the deviation of $g^{(2)}_{\rm opt}(0)$ from 1 according to Eq. (17) will be 2.5 per mille. Further improvements on g_0 and κ are expected using new designs and fabrication methods, so that reaching a signal of $g^{(2)}_{\rm opt}(0) - 1$ on the order of a few percent is a realistic prospect for the near future (cf. Fig. 3).

IX. OUTLOOK: TOWARDS THE SINGLE-PHOTON STRONG-COUPLING REGIME

Our linearized model is strictly valid only for $g_0/\kappa \ll 1$. We can, however, expect qualitative agreement to some extent even for larger g_0/κ. The deviations of F from Eq. (13) in this regime are plotted in Fig. 4(a). Strongly sub-Poissonian states with small limit cycle amplitude $\langle\hat{n}\rangle$ feature a negative Wigner function [23]. As discussed above $\langle\hat{n}\rangle \sim (\kappa/g_0)^2$. It is therefore reasonable to expect negative mechanical Wigner density with g_0/κ approaching the single-photon strong-coupling regime. As depicted in Fig. 4(b) we confirm this numerically. All numerical calculations were done with QUTIP [46,47] (see Appendix).

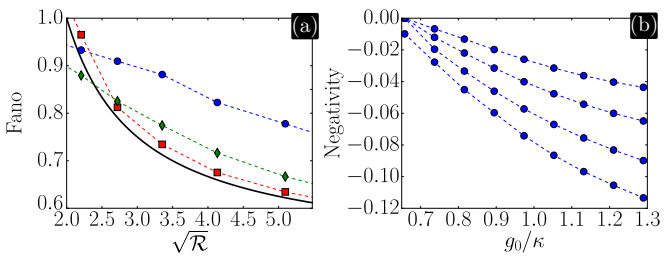

FIG. 4. (Color online) (a) Comparison of analytical results (black solid line) from Eq. (13) to numerical results for Fano factor F with increasing $g_0/\kappa = 0.25, 0.5, 1$ (square, diamond, circle). The parameter $g_0E/\kappa^2 = 0.04$ is fixed to stay well inside the regime of validity of the adiabatic elimination. In this plot $\bar{n} = 0$ but for finite temperature the agreement of numerics with Eq. (13) is equally good. (b) Negativity (quotient of smallest and largest value) of the mechanical oscillator's Wigner function in steady state calculated with QuTiP's steady state solver. The bath occupation is $\bar{n} = 0.25, 0.5, 1, 2$ for the increasing curves. The driving field $E = 0.07\kappa$ is constant in both plots, to stay well in the regime of $n_{\rm ph} \ll 1$ for numerical simplicity. Each point in (b) is optimized over $\mathcal{R}$ by varying γ. All units in this figure are dimensionless.

X. CONCLUSION

Using an optomechanical setup with two optical modes brings experimental demonstration of both sub-Poissonian phonon statistics and optomechanically induced phonon and photon antibunching in reach of today's technology. For parameters approaching the single-photon strong-coupling regime the limit cycle states can even feature a negative mechanical Wigner function.

ACKNOWLEDGMENTS

This work was funded by the Centre for Quantum Engineering and Space-Time Research (QUEST) at the Leibniz University of Hannover and by the European Community (FP7-Programme) through iQUOEMS (Grant Agreement No. 323924). We acknowledge the support of the cluster system team at the Leibniz University of Hannover in the production of this work.

APPENDIX A: CHARACTERIZATION OF PHONON STATISTICS

The phonon statistics is commonly characterized by the Fano factor

$$F = \langle \Delta \hat{n}^2 \rangle / \langle \hat{n} \rangle, \tag{A1}$$

and the second order coherence function $g^{(2)}(t)$ at time $t = 0$,

$$g^{(2)}(0) = \langle c^\dagger c^\dagger c c \rangle / \langle \hat{n} \rangle^2 = 1 + (F - 1)/\langle \hat{n} \rangle, \tag{A2}$$

which gives information on the temporal correlations of the phonons ($g^{(2)}(0) > 1$ and $g^{(2)}(0) < 1$ corresponding to bunching and antibunching, respectively [48]). The Fano factor F can be inferred from $g^{(2)}(0)$ through (1), and F smaller (greater) than 1 also indicates sub- (super-) Poissonian statistics. In [18] $g^{(2)}(0) \approx 1$ was achieved, verifying the coherent nature of the mechanical oscillations in their setup. For comparison, the Poissonian statistics of a (classical) coherent state imply $F = 1$ and $g^{(2)}(0) = 1$, while a thermal state would have $g^{(2)}(0) = 2$.

APPENDIX B: NUMERICAL ANALYSIS

Numerically we calculated the steady state of the system using QUTIP [46,47], the Quantum Toolbox in Python. For Fig. 4(b), where the mechanical amplitudes are small due to the large g_0/κ, the Hilbert space has moderate size and we used a direct steady state solver for density matrices. For Fig. 4(a) the Hilbert space is (in general) too large for this and we had to use Monte Carlo trajectories [49–51] for the wave function and average over many runs to obtain a density matrix. Each trajectory $|\psi_j(t)\rangle$ had a coherent state with random, independent and identically distributed Gaussian amplitudes, $\xi_j \sim \mathcal{N}(\zeta, 1)$ around the analytical steady state amplitude ζ_0 [fulfilling $|\zeta_0|^2 = (\frac{\kappa}{2g_0})^2(\sqrt{\mathcal{R}} - 1)$; cf. the main text] as the initial state for the oscillator. Coherent states with amplitudes given by the best analytical result, $\beta_0 = \frac{E\kappa}{2h_{\zeta_0}}$, $\alpha_0 = -i\frac{Eg_0\zeta_0^*}{h_{\zeta_0}}$, were chosen as the initial state for the optical modes. The system was then evolved according to the master equation

$$\dot{\rho} = -i[H, \rho] + L\rho \tag{B1}$$

with the Hamiltonian

$$H_I = iE(b^\dagger - b) + g_0(ab^\dagger c + a^\dagger b c^\dagger) \tag{B2}$$

and the Lindblad operator $L = L_a + L_b + L_m$, where

$$L_a\rho = \kappa a\rho a^\dagger - \frac{\kappa}{2}a^\dagger a\rho - \frac{\kappa}{2}\rho a^\dagger a, \tag{B3}$$

$$L_b\rho = \kappa b\rho b^\dagger - \frac{\kappa}{2}b^\dagger b\rho - \frac{\kappa}{2}\rho b^\dagger b, \tag{B4}$$

$$L_m = \gamma c\rho c^\dagger - \frac{\gamma}{2}c^\dagger c\rho - \frac{\gamma}{2}\rho c^\dagger c. \tag{B5}$$

The calculation for each trajectory was done in a displaced frame around the (analytically expected) mean amplitude of the mechanical oscillator and cavity modes, in order to reduce the required numerical Hilbert space dimension. Finally we averaged after an evolution time τ over all trajectories to obtain a density matrix $\sigma = \sum_j |\psi_j(\tau)\rangle\langle\psi_j(\tau)|$. With this density matrix we calculated the mean values $\langle \hat{n} \rangle_\sigma$ and $\langle \hat{n}^2 \rangle_\sigma$, which in turn give the Fano factor F and the second order coherence function $g^{(2)}(0)$ according to Eqs. (A1) and (A2). The evolution time was chosen as $\tau = 5/\gamma$ so that both mean values $\langle \hat{n} \rangle_\sigma$ and $\langle \hat{n}^2 \rangle_\sigma$ had already relaxed to steady state while the phase has still not diffused away too far from ζ_0. In this time frame a small Hilbert space around the mean mechanical amplitude was sufficient for the simulation.

[1] M. Aspelmeyer, T. J. Kippenberg, and F. Marquardt, in *Cavity Optomechanics*, edited by M. Aspelmeyer, T. J. Kippenberg, and F. Marquardt (Springer, Berlin, 2014).

[2] M. Aspelmeyer, T. J. Kippenberg, and F. Marquardt, Rev. Mod. Phys. **86**, 1391 (2014).

[3] J. D. Teufel, T. Donner, D. Li, J. W. Harlow, M. S. Allman, K. Cicak, A. J. Sirois, J. D. Whittaker, K. W. Lehnert, and R. W. Simmonds, Nature (London) **475**, 359 (2011).

[4] J. Chan, T. P. M. Alegre, A. H. Safavi-Naeini, J. T. Hill, A. Krause, S. Gröblacher, M. Aspelmeyer, and O. Painter, Nature (London) **478**, 89 (2011).

[5] E. Verhagen, S. Deléglise, S. Weis, A. Schliesser, and T. J. Kippenberg, Nature (London) **482**, 63 (2012).

[6] T. A. Palomaki, J. W. Harlow, J. D. Teufel, R. W. Simmonds, and K. W. Lehnert, Nature (London) **495**, 210 (2013).

[7] K. W. Murch, K. L. Moore, S. Gupta, and D. M. Stamper-Kurn, Nat. Phys. **4**, 561 (2008).

[8] T. P. Purdy, R. W. Peterson, and C. A. Regal, Science **339**, 801 (2013).

[9] T. A. Palomaki, J. D. Teufel, R. W. Simmonds, and K. W. Lehnert, Science **342**, 710 (2013).

[10] T. Carmon, H. Rokhsari, L. Yang, T. J. Kippenberg, and K. J. Vahala, Phys. Rev. Lett. **94**, 223902 (2005).

[11] M. Tomes and T. Carmon, Phys. Rev. Lett. **102**, 113601 (2009).
[12] I. S. Grudinin, A. B. Matsko, and L. Maleki, Phys. Rev. Lett. **102**, 043902 (2009).
[13] I. S. Grudinin, H. Lee, O. Painter, and K. J. Vahala, Phys. Rev. Lett. **104**, 083901 (2010).
[14] G. Bahl, J. Zehnpfennig, M. Tomes, and T. Carmon, Nat. Commun. **2**, 403 (2011).
[15] G. Anetsberger, E. M. Weig, J. P. Kotthaus, and T. J. Kippenberg, C. R. Phys. **12**, 800 (2011).
[16] S. Zaitsev, A. K. Pandey, O. Shtempluck, and E. Buks, Phys. Rev. E **84**, 046605 (2011).
[17] O. Suchoi, K. Shlomi, L. Ella, and E. Buks, Phys. Rev. A **91**, 043829 (2015).
[18] J. D. Cohen, S. M. Meenehan, G. S. MacCabe, S. Gröblacher, A. H. Safavi-Naeini, F. Marsili, M. D. Shaw, and O. Painter, Nature (London) **520**, 523 (2015).
[19] D. A. Rodrigues and A. D. Armour, Phys. Rev. Lett. **104**, 053601 (2010).
[20] A. D. Armour and D. A. Rodrigues, C. R. Phys. **13**, 440 (2012).
[21] J. Qian, A. A. Clerk, K. Hammerer, and F. Marquardt, Phys. Rev. Lett. **109**, 253601 (2012).
[22] P. D. Nation, Phys. Rev. A **88**, 053828 (2013).
[23] N. Lörch, J. Qian, A. Clerk, F. Marquardt, and K. Hammerer, Phys. Rev. X **4**, 011015 (2014).
[24] P. D. Nation, J. R. Johansson, M. P. Blencowe, and A. J. Rimberg, Phys. Rev. E **91**, 013307 (2015).
[25] A. H. Safavi-Naeini and O. Painter, New J. Phys. **13**, 013017 (2011).
[26] M. Ludwig, A. H. Safavi-Naeini, O. Painter, and F. Marquardt, Phys. Rev. Lett. **109**, 063601 (2012).
[27] X. Xu, M. Gullans, and J. M. Taylor, Phys. Rev. A **91**, 013818 (2015).
[28] P. Kómár, S. D. Bennett, K. Stannigel, S. J. M. Habraken, P. Rabl, P. Zoller, and M. D. Lukin, Phys. Rev. A **87**, 013839 (2013).
[29] P. Rabl, Phys. Rev. Lett. **107**, 063601 (2011).
[30] A. Nunnenkamp, K. Børkje, and S. M. Girvin, Phys. Rev. Lett. **107**, 063602 (2011).
[31] V. Braginsky, S. Strigin, and S. Vyatchanin, Phys. Lett. A **287**, 331 (2001).
[32] X. Chen, C. Zhao, S. Danilishin, L. Ju, D. Blair, H. Wang, S. P. Vyatchanin, C. Molinelli, A. Kuhn, S. Gras, T. Briant, P.-F. Cohadon, A. Heidmann, I. Roch-Jeune, R. Flaminio, C. Michel, and L. Pinard, Phys. Rev. A **91**, 033832 (2015).
[33] H. Wu, G. Heinrich, and F. Marquardt, New J. Phys. **15**, 123022 (2013).
[34] S. L. Danilishin, S. P. Vyatchanin, D. G. Blair, J. Li, and C. Zhao, Phys. Rev. D **90**, 122008 (2014).
[35] L. Ju, C. Zhao, Y. Ma, D. Blair, S. L. Danilishin, and S. Gras, Classical Quantum Gravity **31**, 145002 (2014).
[36] H. Wang, Z. Wang, J. Zhang, S. K. Özdemir, L. Yang, and Y.-X. Liu, Phys. Rev. A **90**, 053814 (2014).
[37] H. Jing, S. K. Özdemir, X.-Y. Lü, J. Zhang, L. Yang, and F. Nori, Phys. Rev. Lett. **113**, 053604 (2014).
[38] A. Mari, A. Farace, and V. Giovannetti, arXiv:1407.8364.
[39] We adopt the convention from the review [1] that κ and γ are energy decay rates. Correspondingly, amplitudes decay at $\kappa/2$ and $\gamma/2$.
[40] A. H. Safavi-Naeini, J. T. Hill, S. Meenehan, J. Chan, S. Gröblacher, and O. Painter, Phys. Rev. Lett. **112**, 153603 (2014).
[41] S. M. Meenehan, J. D. Cohen, S. Gröblacher, J. T. Hill, A. H. Safavi-Naeini, M. Aspelmeyer, and O. Painter, Phys. Rev. A **90**, 011803 (2014).
[42] I. Wilson-Rae, N. Nooshi, W. Zwerger, and T. J. Kippenberg, Phys. Rev. Lett. **99**, 093901 (2007).
[43] F. Marquardt, J. P. Chen, A. A. Clerk, and S. M. Girvin, Phys. Rev. Lett. **99**, 093902 (2007).
[44] J. Chan, A. H. Safavi-Naeini, J. T. Hill, S. Meenehan, and O. Painter, Appl. Phys. Lett. **101**, 081115 (2012).
[45] H. Sekoguchi, Y. Takahashi, T. Asano, and S. Noda, Opt. Express **22**, 916 (2014).
[46] J. R. Johansson, P. D. Nation, and F. Nori, Comput. Phys. Commun. **183**, 1760 (2012).
[47] J. Johansson, P. Nation, and F. Nori, Comput. Phys. Commun. **184**, 1234 (2013).
[48] H. J. Kimble, M. Dagenais, and L. Mandel, Phys. Rev. Lett. **39**, 691 (1977).
[49] R. Dum, P. Zoller, and H. Ritsch, Phys. Rev. A **45**, 4879 (1992).
[50] J. Dalibard, Y. Castin, and K. Mølmer, Phys. Rev. Lett. **68**, 580 (1992).
[51] K. Mølmer, Y. Castin, and J. Dalibard, J. Opt. Soc. Am. B **10**, 524 (1993).